

Necdin enhances muscle reconstitution of dystrophic muscle by vessel-associated progenitors, by promoting cell survival and myogenic differentiation

P Pessina^{1,5}, V Conti^{1,5}, R Tonlorenzi², T Touvier³, R Meneveri¹, G Cossu^{2,4} and S Brunelli^{*1,2}

Improving stem cell therapy is a major goal for the treatment of muscle diseases, where physiological muscle regeneration is progressively exhausted. Vessel-associated stem cells, such as mesoangioblasts (MABs), appear to be the most promising cell type for the cell therapy for muscular dystrophies and have been shown to significantly contribute to restoration of muscle structure and function in different muscular dystrophy models. Here, we report that melanoma antigen-encoding gene (MAGE) protein necdin enhances muscle differentiation and regeneration by MABs. When necdin is constitutively overexpressed, it accelerates their differentiation and fusion *in vitro* and it increases their efficacy in reconstituting regenerating myofibres in the α -sarcoglycan dystrophic mouse. Moreover, necdin enhances survival when MABs are exposed to cytotoxic stimuli that mimic the inflammatory dystrophic environment. Taken together, these data demonstrate that overexpression of necdin may be a crucial tool to boost therapeutic applications of MABs in dystrophic muscle.

Cell Death and Differentiation (2012) 19, 827–838; doi:10.1038/cdd.2011.160; published online 18 November 2011

Adult mammalian skeletal muscle is a stable tissue with slow turnover. Nonetheless, it has the ability to complete a rapid and extensive regeneration in response to severe damage generated by direct trauma or genetic defects. Local cues lead to the activation of quiescent myogenic precursors, the satellite cells, that form new myofibers and reconstitute a contractile function.¹ A fraction of activated cells returns to a quiescent state, to maintain a more or less constant pool of satellite cells. This self-maintenance mechanism cannot, however, compensate for the chronic loss of myonuclei throughout lifetime, as reflected by the reduction in satellite cell number with aging, or by their depletion due to continuous activation of muscle repair in dystrophic muscles.² Indeed, in the most severe forms of muscular dystrophy, such as Duchenne muscular dystrophy (DMD), muscle regeneration is progressively exhausted, leading the patient to complete paralysis and death. Therapeutic approaches based on the exogenous stem cell administration have been proposed with success in animal models of the disease. In particular, the mesoangioblasts (MABs)³ are a population of vessel-associated stem cells that have been shown to contribute to muscle repair when transplanted in dystrophic mice and dogs.^{4,5}

Despite the identification of MABs as potential sources of skeletal muscles, and the experimental evidence that they can be used to support *in-vivo* skeletal myogenesis, the molecular mechanism regulating their growth, survival and differentiation into skeletal muscle remains largely unexplored. Design-

ing tools to boost these processes may be a crucial step toward the optimization of cell therapy, and many genes and molecules are now being investigated to manipulate their fate.

Among these molecules, necdin may be one ideal candidate. Necdin (Ndn) is a member of melanoma antigen-encoding gene (MAGE) protein family.⁶ It is a maternally imprinted gene that maps on a chromosomal region known to be deleted in patients suffering from the Prader–Willi syndrome (PWS).⁷ Necdin null mice exhibit some of the features of PWS patients, and the absence of necdin impairs differentiation and maturation of hypothalamic neurons.^{8,9}

In skeletal muscle, necdin has a pivotal role in tissue differentiation and maintenance.^{10,11} In particular, we provided the first evidence that this protein is required for proper myoblast differentiation, for the normal postnatal muscle fiber growth, and for the efficient repair upon muscle injury.¹⁰ We showed that necdin acts at different levels: it cooperates with MyoD to promote the transcriptional activation of myogenin; in addition, it exerts a pro-survival, anti-apoptotic action counteracting the cytotoxic effect of several apoptotic agents.¹⁰ Furthermore, we recently showed, in a mouse model and in human patients, that necdin counteracts muscle wasting specifically induced by cachexia, a pathology in which atrophy is associated with tumor load.^{12,13} In this context, necdin exerts its protecting effect by interfering with tumor necrosis factor alpha (TNF α)-activated signaling at various levels and it is associated with a regenerative response of the muscle to wasting.

¹Department of Experimental Medicine, University of Milano-Bicocca, Monza, Italy; ²Division of Regenerative Medicine, H. San Raffaele Scientific Institute, Milan, Italy; ³E. Medea Scientific Institute, Lecco, Italy and ⁴Department of Biology, University of Milano, Milan, Italy

*Corresponding author: S Brunelli, Department of Experimental Medicine, University of Milano-Bicocca, 20052 Monza, Italy and Division of Regenerative Medicine, H. San Raffaele Scientific Institute, 20132 Milan, Italy. Tel: +39 026 448 8308; Fax: +39 022 643 5066; E-mail: brunelli.silvia@hsr.it

⁵These authors contributed equally to this work.

Keywords: necdin; muscle dystrophy; stem cells; apoptosis

Abbreviations: Ab, antibody; α SMA, alpha-smooth muscle actin; α -SG, alpha-sarcoglycan; DMD, Duchenne muscular dystrophy; GFP, green fluorescent protein; MABs, mesoangioblasts; PDGFR, platelet-derived growth factor receptor; TA, tibialis anterior; TGF β , transforming growth factor beta; TNF α , tumor necrosis factor alpha
Received 07.3.11; revised 03.10.11; accepted 07.10.11; Edited by R De Maria; published online 18.11.11

These evidences prompted us to investigate whether necdin function could be exploited to improve the performance of vessel-associated stem/progenitor cells in dystrophic skeletal muscle regeneration. We demonstrate here that necdin is indeed able to accelerate and enhance myogenic differentiation of MABs and to increase cell survival, thus leading to a more efficient reconstitution of the dystrophic muscle.

Results

Characterization of necdin overexpressing MABs. We isolated MABs from biopsies of muscles of adult (6-month old) C57 mice exactly according to Tonlorenzi *et al.*¹⁴ (Figure 1a). Proliferating MABs (wt MABs) express very low level of necdin, therefore to study its role in these cells we generated a cell line that overexpresses necdin constitutively: we produced a lentiviral vector expressing necdin under the constitutive PGK promoter and eGFP under the CMV promoter in opposite orientation, to infect wt MABs (NDNMABs) (Figure 1b). As a control, we transduced the same cells with the lentiviral vector expressing only eGFP (GFPMABs). Cells were fluorescence-activated cell sorting (FACS) sorted for the GFP expression (around 80% of the total number of cells did express GFP) and after two passages both NDNMABs and GFPMABs express high level of GFP fluorescent signal by immunofluorescence or FACS analysis (Figure 1b and not shown). Quantitative PCR (qPCR) analysis show that NDNMABs express *necdin* around 0.018-fold respect to *GAPDH* and >3000 folds respect to GFPMABs (Figure 1c; Supplementary Figure 1A). Western blot analysis shows indeed a greater expression of necdin in NDNMABs, respect to GFPMABs (Figure 1d).

Proliferation curve demonstrated that all cells, transduced or not, grow at the same rate (Figure 1e).

FACS, RT-PCR and qPCR analysis confirmed that the three populations retained MAB markers (*CD34*, *Sca1*, $\alpha 7$ integrin) and express pericyte markers (*NG2*, *PDGFR* and *alpha-smooth muscle actin* (α SMA)), without significant differences (Figures 1f–h; Supplementary Figure 1B). Likewise, none express endothelial markers, such as *VE cadherin*, nor *Pax7*, marker of satellite cell-derived myoblasts (Figure 1g; Supplementary Figure 1B).

MABs have been demonstrated to differentiate efficiently in different cell types. We, therefore, tested the ability of GFPMABs and NDNMABs to respond to smooth muscle and adipogenic differentiation cues. Induction by transform-

ing growth factor beta (TGF β) led to a high and comparable smooth muscle differentiation frequency in the two populations as seen by the presence of a comparable number of α SMA-positive cells with smooth muscle morphology (Figures 2a and b), and by the increased expression of *smooth muscle myosin* (smMHC) and *Smoothelin*, as differentiation proceeds (Figure 2c). We also show that the levels of *Msx2*, a gene we have previously described to cooperate with necdin in smooth muscle differentiation of MABs,¹⁵ do indeed increase over time (Figure 2c).

After treatment with an adipogenesis inducing medium, NDNMABs showed a number of terminally differentiated, Oil Red-positive cells, that is comparable to that of GFPMABs (Figures 2d and e), but interestingly NDNMAB cells expressed a decreased level of adipogenic markers (AP2 and PPAR γ) at all time points (Figure 2f), suggesting that Necdin slows adipogenic differentiation of MABs.

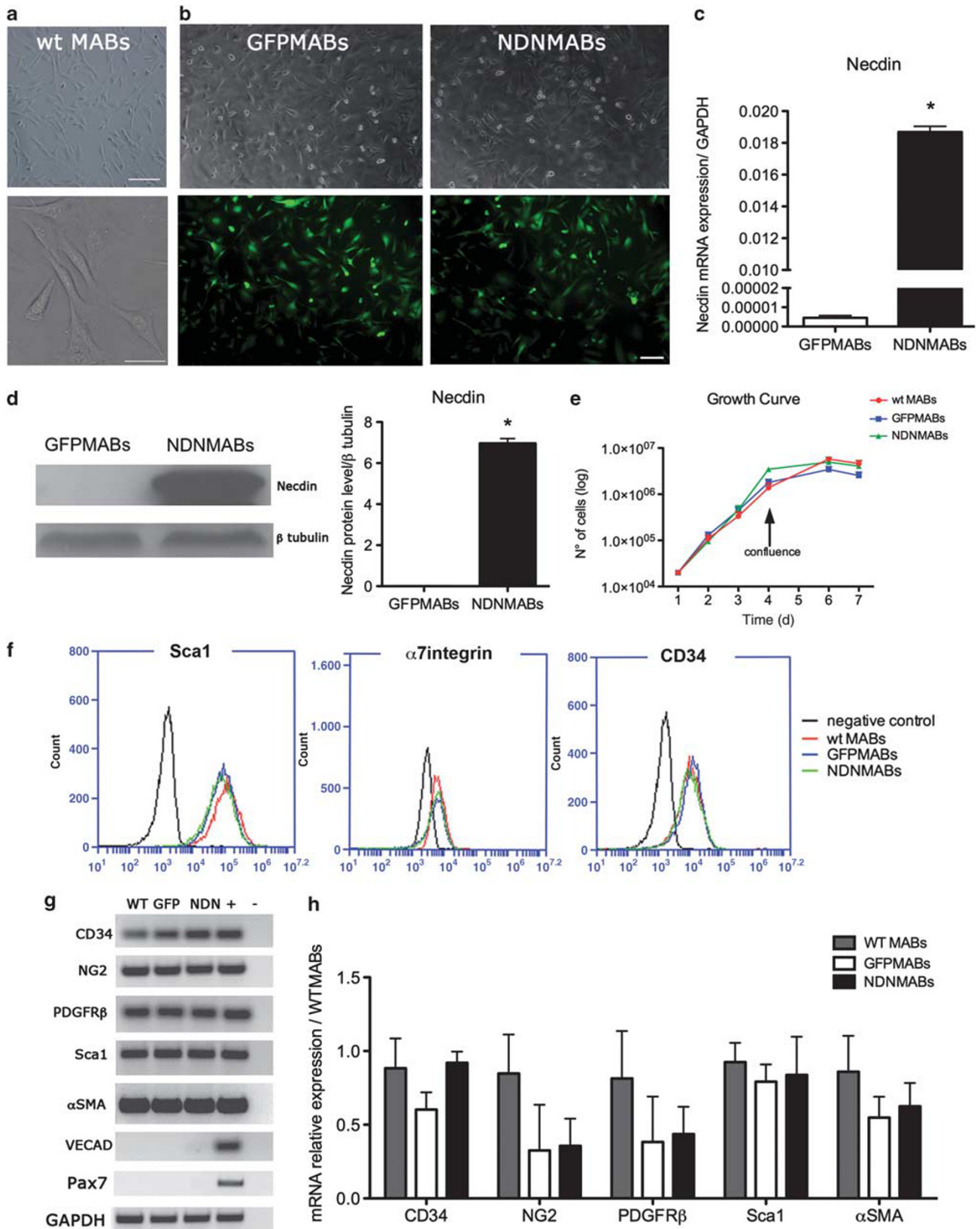
Necdin accelerates MAB cells myogenic differentiation and fusion.

Unlike their embryonic counterpart, MABs derived from adult muscle are able to differentiate in skeletal muscle cells spontaneously, without the need of co-culture with myoblasts and yet they differ from satellite cells because do not express *Pax7*^{14,16} (Figure 1g; Supplementary Figure 1B). Skeletal muscle differentiation was induced by culturing NDNMABs and GFPMABs in muscle-differentiation medium (Figure 3a) and fusion index was calculated to compare their differentiation potential: NDNMABs showed a higher fusion index (NDNMABs: 54%; GFPMABs: 26%), with the progressive appearance of an increased number of myotubes with more nuclei over time, and in particular with >10 nuclei at 6 days (Figures 3b and c).

Enhanced differentiation potential of MABs overexpressing necdin may depend on a different level of expression of myogenic factors leading to an increased expression of muscle-specific cytoskeletal proteins and/or decreased cell death. We first analyzed the expression of *MyoD*, *Myogenin* and *Myosin Heavy Chain* during a time course skeletal muscle differentiation.

Protein and RNA were extracted from GFPMABs and NDNMABs at the beginning of differentiation (T0) and after 3 (T3) and 6 (T6) days. The increased fusion index we observed in NDNMABs was accompanied by increased expression of *Myogenin* and *MyHC*, both at RNA and at protein levels (Figures 3d–f), indicating that necdin accelerates myogenic differentiation by promoting the expression of myogenic factor and then of specific cytoskeletal proteins.

Figure 1 Generation and characterization of MABs overexpressing necdin. (a) Phase-contrast morphology of proliferating adult-derived MABs (wt MABs). Top and bottom images show different magnifications. Scale bar: 100 μ m (top) and 50 μ m (bottom). (b) MABs were transduced with a recombinant lentivirus expressing only GFP (GFPMABs) (left column) as a control or with recombinant lentivirus to overexpress necdin constitutively (NDNMABs) (right column). GFP fluorescence was evaluated 24 h after the infection. Top row: bright field images; bottom row: fluorescence microscopy images. Scale bar: 100 μ m. (c) Necdin mRNA level was measured by qPCR and expressed as fold increase versus *GAPDH*. Error bars represent S.E.M. of five independent experiments; * $P < 0.001$ versus GFPMABs. (d) Representative western blot analysis of necdin expression in GFPMABs and NDNMABs (left). Results from five independent experiments were quantified by densitometry analysis (right) and expressed as fold increase over β -tubulin. * $P < 0.05$ versus GFPMABs. (e) Growth curves of wt MABs, GFPMABs and NDNMABs plotted on a logarithmic scale: the lines are for the most part overlapping, indicating that there was no significant change in the growth rates of the newly generated MAB lines compared with wt MABs. Viable cells were counted every 24 h for 7 days. Results were expressed as mean \pm S.E.M. of duplicate samples of five independent experiments. (f) Flow cytometric analysis of the three lines of MABs using SCA1, $\alpha 7$ integrin and CD34 antibodies. Black line is a negative control. (g) RT-PCR and (h) qPCR on proliferating cells using primers specific for typical MAB markers to compare wt MABs (wt), GFPMABs (GFP) and NDNMABs (NDN). In (h), all data points were calculated in triplicate as gene expression relative to the expression of WTMABs. Data are represented as the mean \pm S.E.M. of five independent experiments



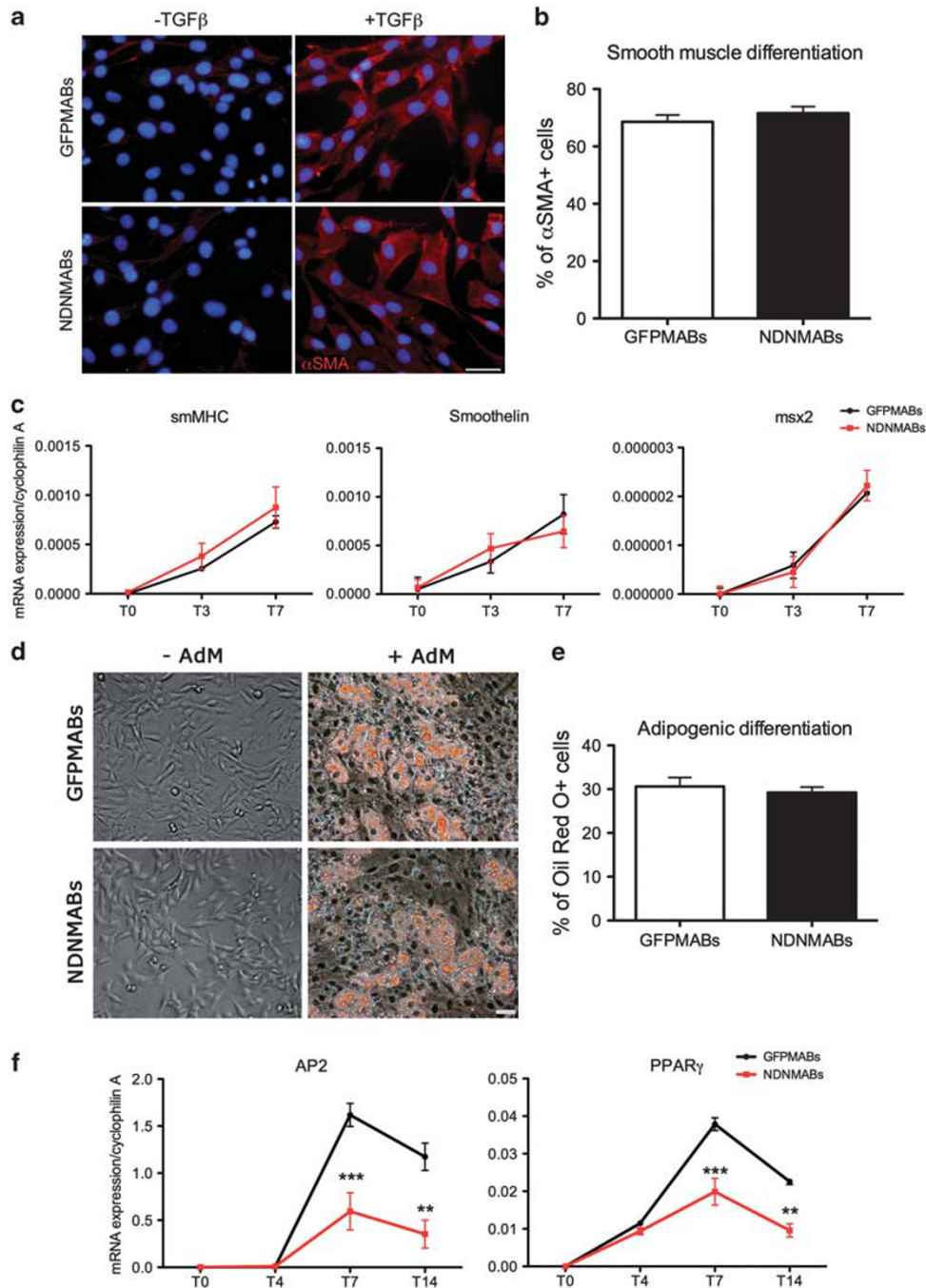


Figure 2 Necdin partially influence adipogenic but not smooth muscle differentiation of MABs. (a) Smooth muscle differentiation was induced by treating MABs with 5 ng/ml of TGF β for 7 days. Immunofluorescence with an antibody specific for α SMA (red) was performed on control and TGF β -treated GFPMABs (top) and NDNMABs (bottom). Nuclei were stained with Hoechst (blue). Scale bar: 100 μ m. (b) Histogram representing the percentage of α SMA-positive TGF β -treated MABs over the total number of cells. An average value was determined by counting cells in at least 10 microscopic fields (150–190 cells/field). Results were expressed as mean \pm S.E.M. of five independent experiments. (c) qPCR on cells undergoing smooth muscle differentiation 0, 3 and 7 days after addition of the differentiation medium (T0, T3 and T7), using primers specific for smMHC, Smoothelin and msx2. All data points were calculated in triplicate as gene expression relative to endogenous cyclophilin A expression. Data are represented as the mean \pm S.E.M. of five independent experiments. (d) Adipogenic differentiation was induced by treating cells with a specifically formulated medium for up to 14 days (AdM). Confirmation of terminal adipogenesis differentiation was made by the Oil Red O staining that highlights lipidic vacuoles in the cytoplasm. Scale bars: 100 μ m. (e) Histogram representing the percentage of MABs positive for Oil Red O staining, over the total number of cells. An average value was determined by counting cells in at least 10 microscopic fields (170–200 cells/field). Results were expressed as mean \pm S.E.M. of five independent experiments. ** $P < 0.005$, *** $P < 0.0005$. (f) qPCR on cells undergoing adipogenic differentiation, at day 0, 4, 7 and T14 after addition of the differentiation medium (T0, T4, T7 and T14) using primers specific for the adipocyte marker aP2 and PPAR γ . All data points were calculated in triplicate as gene expression relative to endogenous cyclophilin A expression. Data are represented as the mean \pm S.E.M. of five independent experiments; ** $P < 0.01$, *** $P < 0.001$

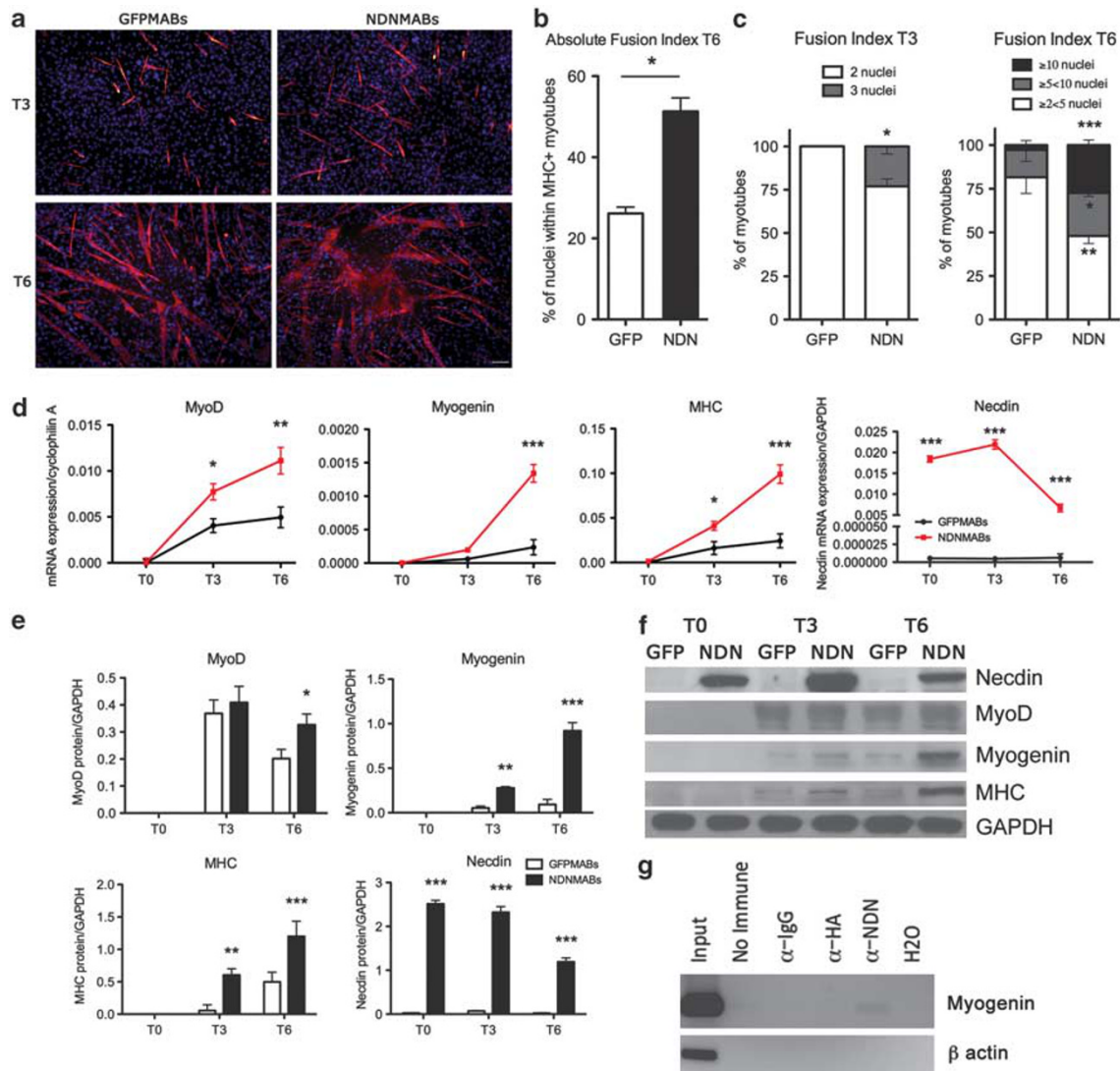


Figure 3 Necdin enhances myogenic differentiation. **(a)** Skeletal muscle differentiation assay. GFPMABs (left column) and NDNMABs (right column) were cultured for 3 (T3, top row) and 6 (T6, bottom row) days in differentiating medium (DMEM with 2% horse serum). Immunofluorescence was performed with a specific antibody against Myosin Heavy Chain (MF20) (red). Nuclei were stained with Hoechst (blue). Scale bar: 100 μ m. **(b)** Absolute fusion index was determined at T6 counting the percentage of MHC-positive nuclei over the total number of nuclei. An average value was determined by counting cells in at least 10 microscopic fields (500–700 cells/field). Results were expressed as mean \pm S.E.M. of five independent experiments. $^*P < 0.05$. **(c)** Relative fusion index was determined at 3 (T3, left) and 6 (T6, right) days in differentiating medium by counting the number of MHC-positive myotubes, according to the number of nuclei per cell. Results were expressed as the mean \pm S.E.M. of five independent experiments. $^*P < 0.05$, $^{**}P < 0.005$, $^{***}P < 0.0005$. **(d)** Time course of skeletal muscle differentiation was evaluated by qPCR analysis for MyoD, Myogenin, MHC and necdin expression in GFPMABs and NDNMABs. All data points were calculated in triplicate as gene expression relative to endogenous cyclophilin A (for MyoD, Myogenin and MHC) or GAPDH (for Necdin) expression. Data are represented as the mean \pm S.E.M. of five independent experiments. $^*P < 0.05$, $^{**}P < 0.01$, $^{***}P < 0.001$. **(e and f)** Western blot analysis with specific antibodies against MyoD, myogenin, MHC and Necdin in GFPMABs and NDNMABs at different time points during skeletal muscle differentiation. GAPDH protein level was used as an internal loading control. Graphs **(e)** show mean values \pm S.E.M. obtained from the ratio of densitometric values of protein/GAPDH bands on the blot of the same experiments. Data are representative of five independent experiments. $^*P < 0.05$, $^{**}P < 0.01$, $^{***}P < 0.001$. The western blot in **(f)** shows a representative experiment. **(g)** Soluble chromatin was prepared from cultures of NDNMABs differentiated for 72 h in differentiating medium, and immunoprecipitated with an antibodies specific for necdin. Parallel extracts were exposed to rabbit IgG and to rabbit HA as control for non-specific precipitation of chromatin. Precipitated genomic DNA was analyzed by PCR, using primers designed to amplify sequences in the myogenin promoter. Input refers to DNA input control in which PCR amplification was performed before immunoprecipitation. A sample where no antibody was used for immunoprecipitation was run in parallel (no Immune)

MyoD RNA but not protein levels appear slightly increased in NDNMABs at T3 and T6. Necdin levels in GFPMABs remain the same over time, while it appears that viral mediated necdin expression in NDNMABs increases at T3 and then decrease at T6, both at RNA and at protein level (Figures 3d–f).

In C2C12 myoblasts, we have described that necdin binds to the myogenin promoter and therefore cooperates to the transcription of this gene.¹⁰ We investigated whether this mechanism of action was conserved in MABs differentiation. Chromatin immunoprecipitation was performed on NDNMABs

as in Deponti *et al.*¹⁰ We found indeed that necdin was equally able to bind this DNA sequence that was precipitated by anti-necdin antibody (Figure 3g), indicating that this maybe one direct mechanism of action leading to enhanced myogenic differentiation of NDNMABs.

Necdin protects MABs from cell death. An important aspect of the acute and chronically damaged muscle is that it originates a pro-apoptotic microenvironment in which cytokines such as TNF α , and reactive oxygen species, generated by both the necrotic fibers and cells of the immune system infiltrating the muscle,¹⁷ that may contribute to the limited effect of myogenic cells transplantation.

Our previous studies revealed that necdin acts as a pro-survival factor in muscle cells.¹⁰ We investigated whether necdin has the same role also on MABs. Proliferating GFPMABs and NDNMABs were exposed either to staurosporine (2 μ M) for 3 h or overnight to the reactive oxygen species arsenic trioxide (As₂O₃) (20 μ M). After treatment, we evaluated cell death by measuring propidium iodide (PI) incorporation by FACS.

Figures 4a and b (Supplementary Figure 2A) shows dot plots relative to representative experiments. Three populations can be clearly distinguished: GFP⁺ PI⁻ cells (live cells); GFP⁺ PI^{low} cells (cells that start to lose the membrane integrity and in which, consequently, the PI is only present in the cytoplasm) and GFP⁻ PI^{high} cells (dead cells that have lost GFP expression because of the complete loss of membrane integrity and in which the PI is intercalated in the DNA).

We analyzed and plotted (Figures 4c and d) the number of dead cells (GFP⁻ PI^{high}) and we observed that NDNMABs showed a 35% increase in cell vitality respect to GFPMABs.

In addition to the marked reduction of the GFP⁻ PI^{high} population, we also observed a reduction in the number of the GFP⁺ PI^{low} population. In particular, after staurosporine treatment, NDNMABs showed a 30% decrease and, after As₂O₃ treatment, a 50% decrease of the apoptosing cell population, if compared with GFPMABs. These data confirmed that overexpressing necdin MABs resist better to the different apoptotic treatments used, thus demonstrating that necdin has a crucial role in cell survival also in vessel-associated myogenic progenitors.

Necdin promotes MAB-mediated muscle reconstitution *in vivo*. These encouraging results *in vitro* led us to investigate whether necdin could optimize MABs contribution to muscle repair *in vivo*, in a murine model of muscular dystrophy, the α -sarcoglycan null (α -SG^{-/-}) mice.

We performed intramuscular injections of GFPMABs and NDNMABs in the Tibialis Anterior (TA), quadriceps (QUAD) or gastrocnemius (GASTRO) of 4-month-old α -SG^{-/-} mice. We injected 5×10^5 cells in 50 μ l of physiological solution (TA) and 7×10^5 cells in 70 μ l of physiological solution (QUAD and GASTRO). To have an internal control, we injected GFPMABs in the right muscles and NDNMABs in left muscles of the same mouse.

We first detected the ability of MABs to survive in the inflammatory microenvironment of dystrophic muscles. To this end, we transplanted GFPMABs or NDNMABs in muscles of α -SG^{-/-} mice, we killed them 24 h later and we collected

treated muscles for subsequent experiments (Supplementary Figure 3A).

Since *in-vivo* necrotic MABs, that have lost the GFP expression, cannot be discriminated anymore from other host cells, we focused our analysis on the detection of early and late stages of apoptosis.

We combined TUNEL assay with immunofluorescence against GFP. Counting on muscle serial sections, we demonstrated that muscle transplanted with NDNMABs contained a decreased number of apoptosing TUNEL⁺ GFP⁺ cells, respect to control MABs (Figures 5a and b).

We collected mRNA from muscles injected with MABs and we evaluated the number of surviving and transcriptionally active MABs by qPCR using specific primers for GFP. We normalized the level of GFP messenger in each injected-muscle sample with that corresponding to the total input of injected cells. We demonstrated that muscles treated with NDNMABs showed a greater GFP expression, indicating a higher survival level of these cells, and we can indirectly estimate the number of dead MABs that are no longer detectable in the muscle (Figure 5c).

Moreover, we performed a FACS analysis on single cells dissociated from the transplanted muscles and we evaluated the amount of apoptotic MABs as the number of GFP-positive cells that are also positive for 7-amino-actinomycin D (7AAD). We demonstrated that muscles injected with GFPMABs contained almost double the amount of GFP⁺ 7AAD⁺ respect to NDNMAB-injected muscles (Figures 5d and e; Supplementary Figure 2B).

All these data are in agreement with the *in-vitro* results, indicating that overexpression of necdin confers to MABs a higher resistance to cell death.

We, therefore, determined the ability of these cells to regenerate new muscle fibers by evaluating the restoration of α -SG expression in regenerating fibers. We performed immunofluorescence staining for α -SG on cryosections of TA muscles of α -SG^{-/-} mice treated with intramuscular injections of GFPMABs and NDNMABs and killed 14 days after the injection and of wt or α -SG^{-/-} mice as controls. Sections from mice treated with NDNMABs showed higher number of α -SG-positive fibers (Figure 6a). Some of the MABs that do not contribute to the new regenerating fibers, remain in the interstitial space between fibers, together with other cells, such as macrophages, that infiltrate the dystrophic muscle (Supplementary Figure 3B–C).

Accordingly, muscles treated with NDNMABs showed a higher level of α -SG expression respect to muscles treated with GFPMABs both as RNA, as revealed by real-time PCR analysis (Figure 6b) and as protein, measured by western blot (Figure 6c).

Discussion

There is actually no cure for muscular dystrophies, although many strategies are entering clinical experimentation. Among these, stem cell therapy is an attractive approach and research in this direction has moved very rapidly in the last years. Stem cell populations with myogenic potential can be isolated from multiple regions of the body.^{18,19} Until now,

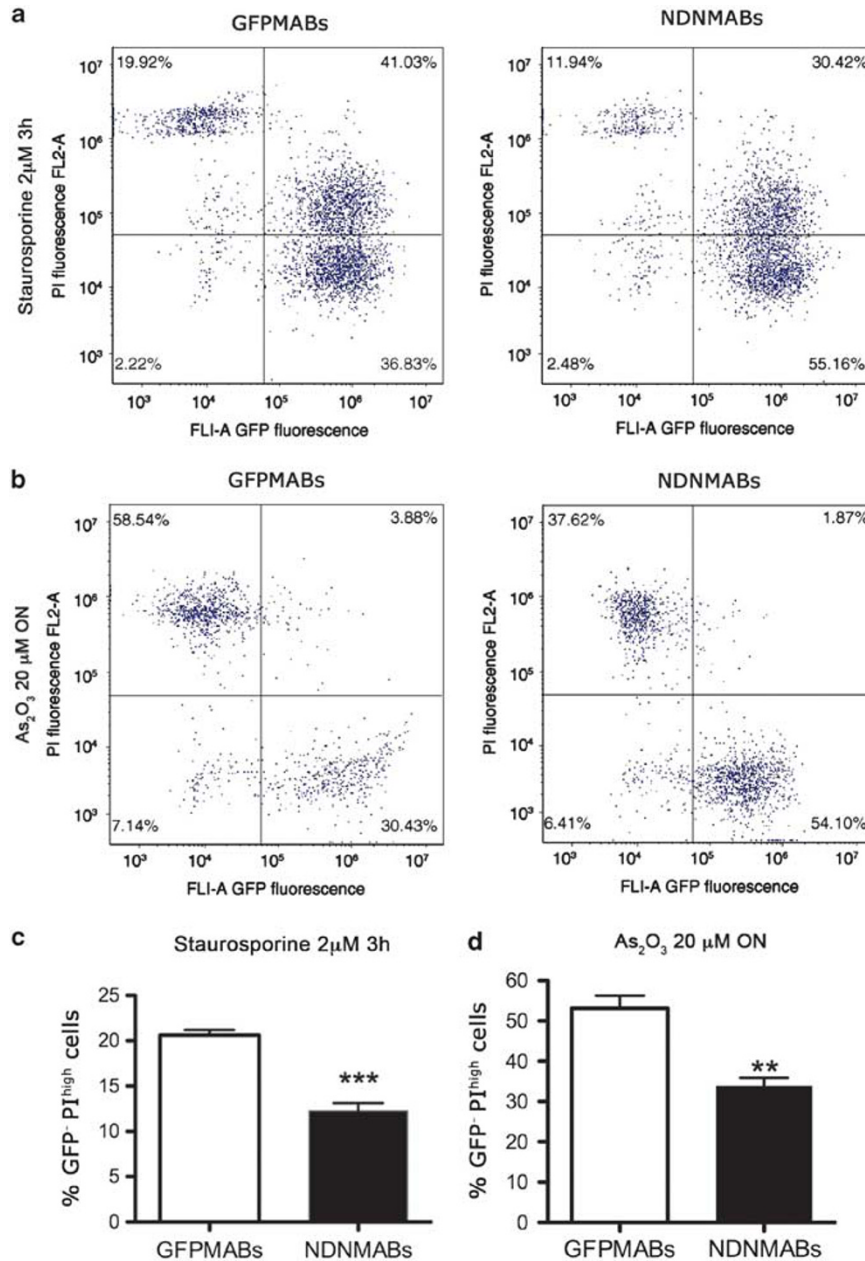


Figure 4 Necdin expression confers an improved cell survival *in vitro*. Cell death of GFPMABs and NDNMABs was induced by treating cells with staurosporine (2 μ M) for 3 h (**a-c**) or As₂O₃ (20 μ M) overnight (**b-d**). Percentage of dead cells (GFP⁻ PI^{high}) and apoptosing cells (GFP⁺ PI^{low}) was evaluated by FACS analysis, measuring PI incorporation. (**a** and **b**) Dot plots relative to representative experiments. (**c** and **d**) Charts representing the number of dead cells (GFP⁻ PI^{high}) after staurosporine (**c**) or As₂O₃ (**d**). Error bars represent mean values \pm S.E.M. of six independent experiments. ** $P < 0.005$, *** $P < 0.0005$

MABs appear to fulfil most of the features required for a clinical use in human patients^{3,14,16} and have shown to significantly contribute to the restoration of the muscle structure and function in mouse and dog models of muscular dystrophy.^{4,5,20} Still protocol optimization for cell therapy is ongoing, and different drug and gene therapy approaches have been investigated to improve their clinical outcome.

For example, the treatment of dystrophic mice with nitric oxide plus NSAIDs²¹ and/or the treatment of MABs with NO, SDF1, S1P or HMGB1 improved to different levels and with different mechanisms either homing or survival of MABs in skeletal muscle, increasing their therapeutic effectiveness.²²⁻²⁵

Here, we demonstrate that the efficacy of MABs cells to reconstitute dystrophic muscle is improved by the expression of the MAGE protein necdin. Importantly when necdin is overexpressed, both the myogenic differentiation and survival of MABs were enhanced both *in vitro* and *in vivo*.

We have previously shown that necdin has an important role in skeletal muscle differentiation and maintenance by satellite-derived myoblasts in different conditions of muscle damage or wasting;^{10,12} therefore, we constitutively overexpressed necdin in adult MABs. We found that necdin, when overexpressed in MABs, causes a higher fusion rate *in vitro*,

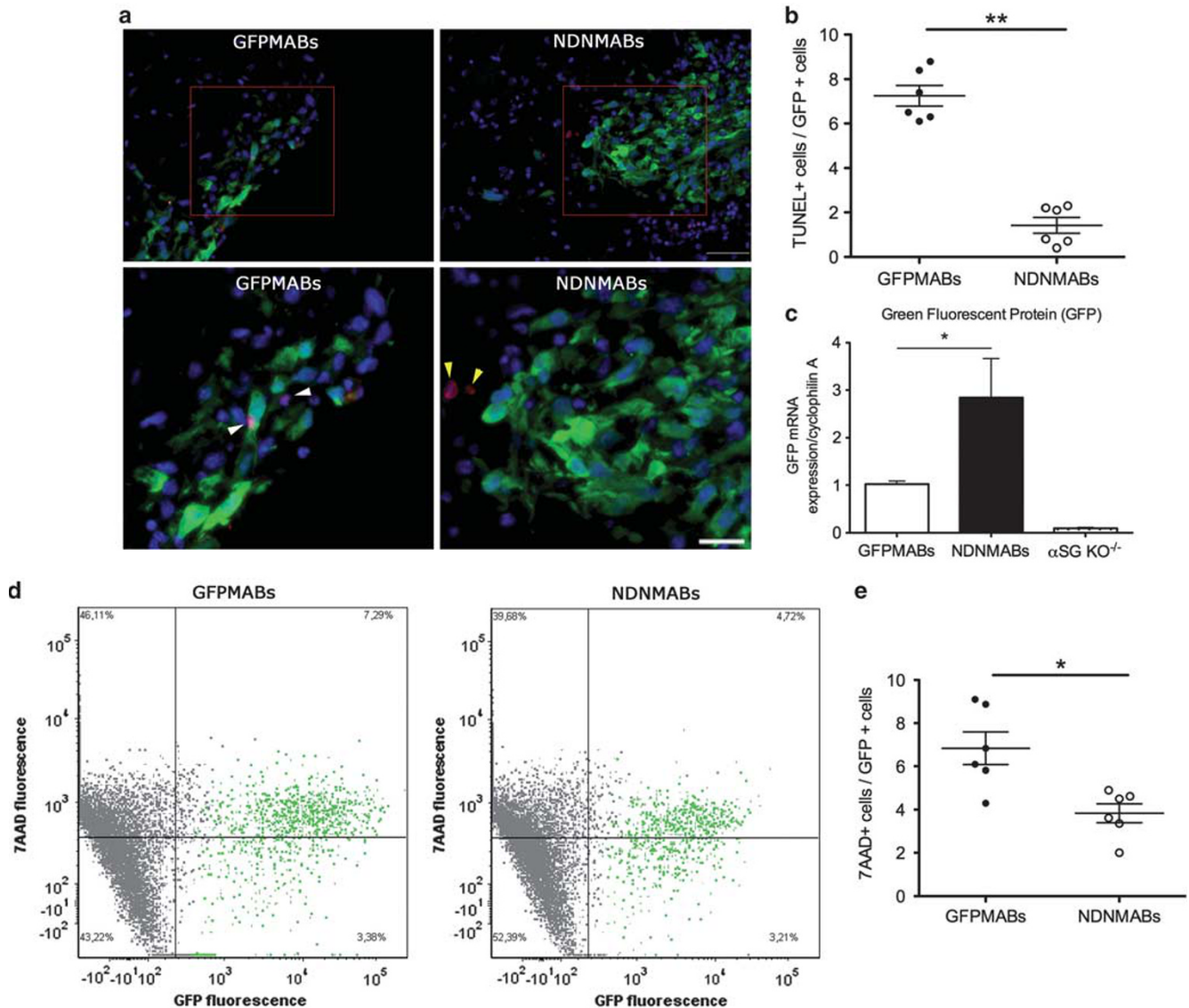


Figure 5 Necdin expression increases engrafted MABs survival *in vivo*. (a and b) 5×10^5 MABs were injected intramuscularly into TA of 4-month-old α -SG^{-/-} mice. After 24 h, muscles were collected and OCT embedded. Cryosections of GFPMAB-injected (left column) or NDNMAB-injected (right column) muscles were stained for TUNEL (red) and Hoechst (blue) and immunofluorescence was performed using a GFP-specific antibody (green). Top and bottom rows show different magnifications. Scale bars: 50 μ m (top) and 25 μ m (bottom). (b) The graph shows the number of TUNEL⁺ GFP⁺ cells over the total number of GFP⁺ cells. An average value was determined by counting cells in at least 10 microscopic fields (100–150 GFP-positive cells/field). Values shown are the mean values \pm S.E.M. of experiments on six animals. ** $P < 0.001$ versus GFPMAB-injected muscles. (c) GFPMABs or NDNMABs (7×10^5) were injected intramuscularly into the gastrocnemius of 4-month-old α -SG^{-/-} mice. After 24 h, muscles were collected and the number of surviving and transcriptionally active MABs was evaluated by qPCR using specific primers for GFP. Data were calculated by comparing the level of GFP messenger in each injected-muscle sample with that corresponding to the total input of injected cells. All data points were calculated in triplicate as gene expression relative to endogenous cyclophilin A expression. Values shown are the mean values \pm S.E.M. of experiments on six animals per group. * $P < 0.05$ versus GFPMAB-injected muscles. (d) Muscles of α -SG^{-/-} mice intramuscularly injected with MABs were digested to single cell suspension and cells were stained with 7AAD. FACS analysis was performed to quantify the amount of apoptotic MABs (7AAD⁺ cells) within the population of the GFP-positive cells. (e) The graph shows the percentage of 7AAD⁺ cells over the total number of GFP⁺ cells. Values shown are the mean values \pm S.E.M. of experiments on six animals. * $P < 0.01$ versus GFPMAB-injected muscles

suggesting that necdin is required to increase their differentiation potential by promoting new myofiber growth and fusion. To understand the molecular mechanisms that regulate this process, we first investigated if necdin could act on transcriptional pathways, as we already demonstrated for satellite-derived myoblasts.¹⁰ In myoblast cultures from the gain of function transgenic mice (MlcNec), increased expression correlates with an increased fusion index and with

changes in the expression of different myogenic markers, including myogenin and sarcomeric myosin. In particular, we found that necdin acts through a transcriptional regulation of myogenin, in cooperation with MyoD. Here, we found that in MABs triggered to differentiate into skeletal muscle, an increased expression of necdin led to an accelerated myogenesis and to a higher rate of fusion. This correlates with higher levels of myogenin and skeletal myosin, suggest-

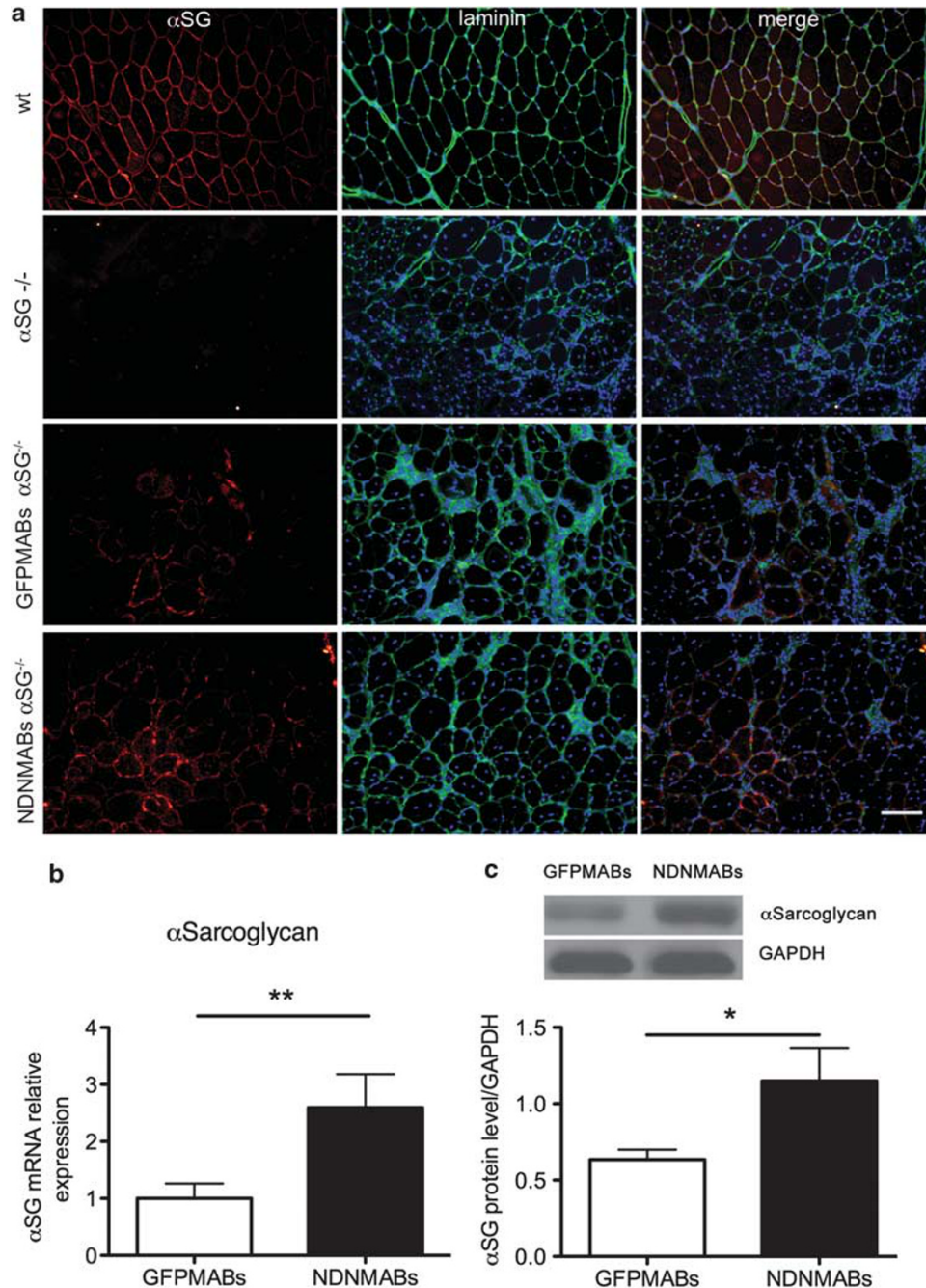


Figure 6 Necdin expression leads to an improved MAB-mediated reconstitution of the dystrophic muscle. (a) Immunofluorescence with specific antibodies for α -SG (red) and laminin (green) on sections of TA of α -SG^{-/-} mice ($n = 21$) killed 14 days after intramuscular injection of 5×10^5 MABs. Nuclei were stained with Hoechst (blue). The panel shows immunofluorescence on TA of wt mouse, α -SG^{-/-} mouse and α -SG^{-/-} mice injected with GFPMABs or NDNMABs. Representative sections are shown. Scale bar: 100 μ m. (b) α -SG expression, evaluated by qPCR, in quadriceps of α -SG^{-/-} mice injected with 7×10^5 GFPMABs or NDNMABs. All data points were calculated in triplicate as α -SG expression relative to muscles injected with GFPMABs. The values indicated in the chart are the mean values \pm S.E.M. of experiments on 14 animals. ** $P < 0.005$ versus GFPMAB-injected muscles. (c) Western blot analysis with an antibody specific for α -SG on muscles of α -SG^{-/-} mice killed 14 days after intramuscular injection of 7×10^5 MABs. GAPDH protein level was used as an internal loading control. Graph shows mean values \pm S.E.M. obtained from the ratio of the densitometric values of protein/GAPDH bands of experiments on 10 animals. The image shows a representative experiment. * $P < 0.01$ versus GFPMAB-injected muscles

ing that necdin have a similar role in controlling the action of myogenic regulatory factors. We indeed demonstrate that this effect may be linked to a direct transcriptional action of necdin, since it is able to bind to the same promoter sequence of the Myogenin gene, as it does in myoblasts.¹⁰

Most importantly necdin did not trigger myogenic differentiation alone, but only when a differentiation stimuli is provided. This is of great importance since ideally the stem cells should differentiate only upon reaching the damaged muscle, where the environment of the remodeling tissue can

trigger myogenic differentiation. Therefore, cells overexpressing necdin, even at very high levels, but in conditions that do not favor differentiation, and in absence of other myogenic regulatory factors behave as controls, in terms of proliferation and expression of specific molecular markers.

Furthermore, the differentiation enhancement is limited to skeletal myogenesis: smooth muscle differentiation is not affected. This is in agreement with what we described previously: necdin is indeed involved in smooth muscle differentiation of MABs but only in combination with the transcription factor *Msx2*,¹⁵ that is not expressed in proliferating MABs, nor GFP-MABs nor NDN-MABs, but that is moderately upregulated upon smooth muscle differentiation stimuli (e.g., TGF β).

We also observed that a similar amount of terminally differentiated adipocytes (Oil Red O-positive cells) are present at the end of the treatment with an adipogenic differentiation medium, whether necdin is overexpressed or not. Interestingly, time course analysis of adipogenic markers shows that overexpression of necdin decreases their levels of expression. Necdin inhibition of adipogenic differentiation of pre-adipocytes has been previously described,^{26,27} but no data are available on the co-factor that may cooperate with necdin in this process, and more experiments will be required to get more insight into this issue. There is evidence that in the aged or dystrophic muscle mesenchymal progenitors distinct from satellite cells contribute to ectopic fat cell formation in degenerating skeletal muscle, in aging or dystrophy.²⁸ It is also still unclear whether this environment could trigger adipogenic conversion of myogenic precursors, therefore leading to an additional muscle loss.²⁹ It would be of great importance to get more insights into the role of necdin in this fate choice, since overexpression of necdin could not only lead to an increased myogenic differentiation of endogenous or transplanted myogenic precursors, but at the same time inhibit their adipogenic differentiation.

Necdin has been also demonstrated to have a role as anti-apoptotic protein. In particular, we demonstrated that necdin interacts both with caspase-3 and caspase-9 pathways in satellite cells.¹⁰ Since the reduced ability of MABs to resist the cytotoxic environment existing in the damaged muscle maybe one of the main reasons for their partial effect, we tested this possibility by exposing MABs to cytotoxic stimuli and found that necdin protects MABs from cell death.

In agreement with these results *in vitro*, we showed that MABs overexpressing necdin, when delivered in α -SG^{-/-} mice, are able to better survive in the cytotoxic dystrophic environment. More interestingly, it provides a greater contribution to muscle repair, as demonstrated by an increased expression of α -SG and restoration of α -SG expressing muscle fibers. We show that some undifferentiated MABs, both GFP-MABs and NDN-MABs, are retained in the interstitium of the dystrophic muscle, where other cells are present, in particular macrophages.¹⁷

We think our results open a new way to manipulate MABs fate. Recently, a Human Artificial chromosome vector (HAC vector) has been manipulated to contain the entire human dystrophin gene including its entire transcriptional regulatory elements (DYS-HAC).³⁰ This DYS-HAC was stably maintained in mice and cultured human cells, and mice derived

from ES containing this HAC were expressing the transgene. This system, whether successfully applied to the MAB-mediated stem cell therapy approach, could be additionally exploited to contain not only dystrophin, but also a series of other genes, to optimize the feature of the stem cells. In this light, necdin could provide transplanted cells with the ability to better survive and to differentiate efficiently when in the appropriate conditions, without interfering with their properties, and to contribute to an optimal skeletal muscle reconstitution.

One critical concern on the use of necdin in the optimization of stem cell therapy is the potential tumorigenic risk. Many proteins of the MAGE family, in particular those belonging to Type I (MAGE A, B and C), are characterized by a wide expression in a variety of malignant tumors, and are being considered as highly attractive targets for cancer immunotherapy.³¹ However, other than this association, little is known regarding their functions in cell activities and in tumor initiation and progression. Necdin is on the other hand a member of Type II proteins that are expressed in normal tissues. Necdin has been also suggested having a role as a tumor suppressor gene.³² Long-term studies on mice overexpressing necdin or on immunodeficient mice injected with cells overexpressing necdin will be certainly required to address this issue.

Detailed studies on the molecular mechanism of the effect of necdin in myogenic stem cells and in general in muscle regeneration are on their way to further enhance its action, which may be a crucial step toward the optimization of cell therapy by MABs or other stem cells.

Materials and Methods

MAB cell culture and *in-vitro* differentiation. MABs were isolated and cultured exactly as previously described in Tonlorenzi *et al.*¹⁴ Specifically, adult-derived murine MABs were isolated from muscular biopsies of a 6-month-old C57BL/6 mouse hind legs. After dissecting both the TA and rinse them in PBS with Ca²⁺-Mg²⁺ to remove residual blood, they were carefully cleaned from adipose and connective tissues, trying to identify portions of interstitial tissue containing small vessels. The fragments were minced in 1–2 mm pieces and transferred onto collagen type I-coated dishes and incubated at 37°C, 5% CO₂ and 5% O₂ in proliferation medium consisting of Dulbecco's modified Eagle's medium (DMEM) supplemented with 20% fetal bovine serum, 2 mM L-glutamine, 1 mM sodium pyruvate, 100 IU/ml penicillin and 100 mg/ml streptomycin. After 5–8 days at 37°C, besides initial outgrowth of adherent cells, mainly consisting of large and flat fibroblasts, MABs could be discerned as small, poorly adhering and very refractile cells. The mixed population was enzymatically dissociated by collagenase/dispase treatment and cloned by limiting dilution in 96-multiwell dishes. After 7–10 days, first clones of cells were distinguishable and propagated in proliferation medium. After few passages most of the clones adopted a large, flat morphology and underwent proliferative senescence. However, few clones retained a small, refractile, morphology with the ability to proliferate for at least 40 passages.

MABs were induced to differentiate to smooth muscle as described in Tagliafico *et al.*³³ and to induce the adipogenic differentiation the STEMPRO Adipogenesis Differentiation Kit (GIBCO, Grand Island, NY, USA) was used, according to the manufacturer's protocol. After 10 days, cells were washed in PBS, fixed in 4% PFA for 5 min at room temperature and subsequently incubated with Oil Red O solution, as previously described.¹⁴ The proportion of cells differentiating in each different cell type was calculated by counting the cells expressing the appropriate differentiation markers against the total number of cells. The average number was determined by counting cells in at least 10 microscopic fields (170–200 cells/field), in at least 5 independent experiments.

MABs derived from adult muscle can spontaneously differentiate into multinucleated skeletal myotubes when cultured onto matrigel-coated plastic support

in differentiation promoting medium (complete medium supplemented with 2% horse serum).

Lentiviral vector preparation and MABs transduction. The control GFP lentiviral vector and the necdin lentiviral vector (in pCCLsin.cPPT.SV40polyA.eGFP.minCMV.hPGK.Wpre) were generated and prepared as described in Deponti *et al.*¹⁰

Viral titer was determined by GFP fluorescence infecting HeLa cells with serial dilution of the virus. The final MOI was 10^7 TU/ml. After 24 h in culture, MABs were transduced with an MOI of 100 in proliferation medium overnight. The next day, the medium was changed and cells were maintained in proliferation medium for one passage and then subjected to FACS for GFP-positive cells.

We generated six different lines overexpressing Necdin and four control lines. Necdin expression in NDNMABs ranged from 0.003- to 0.018-fold GAPDH expression (Supplementary Figure 1A) and expression was 834–4938-fold the expression in GFPMABs. Necdin expression in GFPMABs ranged from 0.000004- to 0.000006-fold GAPDH expression (average Ct, GFPMABs: 31; NDNMABs: 20; GAPDH: 13). Since in a preliminary analysis we did not observe toxicity, and the effect on proliferation, differentiation or survival *in vitro* was similar, we have decided to further characterize a single line for each construct.

Generation of the growth curve. MABs from the different genotypes were seeded at a density of 2×10^3 cells per cm^2 of surface area in 6-well plates or T25 flasks in duplicate. Cell number was assessed by direct cell count and viable cells were judged by Trypan blue dye (Sigma, St. Louis, MO, USA) exclusion. The duplicate plates were counted every 24 h and the results were plotted on a logarithmic scale.

Flow cytometry analysis. The monoclonal antibodies used for this analysis were the following: anti- α 7integrin-PE (MBL), anti-Sca1-APC and anti-CD34-Alexa 647 (eBioscience, San Diego, CA, USA).

MABs were harvested, washed twice with PBS, resuspended in blocking solution (10% FBS in PBS) and incubated for 15 min at room temperature. Subsequently, cells (2×10^5 per tube) were incubated with various combinations of conjugated antibodies for 45 min at 4°C in the dark, according to the manufacturer's recommendations. The background level was estimated by omitting the primary antibody. After PBS washing, cells were fixed in 1% PFA before FACS analysis.

Cell analysis was performed on at least 10 000 events for each sample and determined using the Accuri C6 Flow Cytometer System (Franklin Lakes, NJ, USA) equipped with a blue (488 nm) and a red (640 nm) laser, two scatter detectors, and four fluorescence detectors with interference filters optimized for the detection of FITC, PE, PerCP-Cy5.5 and APC. The analysis was performed using the Accuri CFlow software (Franklin Lakes, NJ, USA). A primary gate based on the physical parameters (forward and side light scatter, FSC and SSC, respectively) was set to exclude dead cells or small debris.

Immunofluorescence. Immunofluorescence on cell cultures and cryosections was performed according to Brunelli *et al.*¹⁵ using antibodies specific for sarcomeric myosin MF20, α -SMA (Sigma), laminin (Abcam, Cambridge, UK), GFP (Chemicon International, Temecula, CA, USA), Necdin (Upstate Biotechnology, Waltham, MA, USA), CD68 (AbD Serotec, Kidlington, UK) and alpha-sarcoglycan (anti-SGCA, Sigma). For fluorescence detection, appropriate secondary antibodies conjugated with either Alexa 488 (green; Invitrogen, Carlsbad, CA, USA) or Alexa 594 (red; Invitrogen) or Alexa 647 (purple, Invitrogen) were used. Nuclei were stained with Hoechst.

To compare the ability of MABs from the different genotypes to fuse and differentiate into multinucleated myotubes, we evaluated both the relative fusion index, counting the number of MHC-positive myotubes, calculated as the number of nuclei per cell, after 3 and 6 days in the differentiating medium, as well as the absolute fusion index, calculated as the percentage of MHC-positive nuclei over the total number of nuclei after 6 days in differentiation medium. An average value was determined by counting cells (500–700 cells/field) in at least 10 microscopic fields. Results were expressed as mean \pm S.E.M. of five independent experiments.

RT-PCR. RNA (1–2 μ g) collected from cells or tissues using RNeasy Mini (or Micro) kit (Qiagen, Germantown, MD, USA) or the TRIzol protocol (Invitrogen) was converted into double-stranded cDNA using the cDNA synthesis kit 'High Capacity Reverse Transcription Kit' (Applied Biosystems, Foster City, CA, USA), according to the manufacturer's instructions.

RT-PCRs were performed using the GoTaq Mix (Promega, Madison, WI, USA) for GAPDH (5'-TTCACCACCATGGAGAAGGC-3' FW; 5'-GGCATGGACTGTGGT-CATGA-3' REV); CD34 (5'-ACCACACCAGCCATCTCAG-3' FW; 5'-TAGATGG-CAGGCTGGACTTC-3' REV); NG2 (5'-ACAAGCGTGGCAACTTTATC-3' FW; 5'-ATAGACTCTTCTCATATTCAT-3' REV); PDGFR β (5'-CCGGAACAAACACACCTTCT-3' FW; 5'-AACATGGGCACGTAATCTATA-3' REV); Sca1 (5'-TTACCCATCTGCCCTCTAA-3' FW; 5'-GGTCTGCAGGAGACTGAGC-3' REV); α SMA (5'-CTGACAGAGGCACCAGTAA-3' FW; 5'-CATCTCCAGAGTCCAGCACA-3' REV); VE cadherin (5'-GTACAGCATCATGCAGGGCG-3' FW; 5'-ATTCGTATCGGATAGTGGGG-3' REV); Pax7 (5'-GACTCGGCTTCTCCATCTC-3' FW; 5'-AGTAGGCTTGCCCGTTCC-3' REV).

Real-time qPCR was carried out with a real-time PCR system (Mx3000P; Stratagene, La Jolla, CA, USA). Each cDNA sample was amplified in triplicate by using the SYBR Green Supermix (Bio-Rad, Hercules, CA, USA) for cyclophilin A (5'-CATACGGTCTCCATCTTTGCC-3' FW; 5'-TGGTGATCTTCTTGCTGGTCTTC-3' Rev), GAPDH (5'-CACCATCTTCCAGGAGCGAG-3' FW; 5'-CC TTCTCCATGGTGGTGA AGAC-3' Rev), Necdin (5'-GGTGAAGGACCAGAAGA GGA-3' FW; 5'-TGGGCATACGGTTGTTAG-3' Rev), CD34 (5'-ACCACACCAGC-CATCTCAG-3' FW; 5'-TAG ATGGCAGGCTGGACTTC-3' Rev), NG2 (5'-ACA AGCGTGGCAACTTTATC-3' FW; 5'-ATAGACTCTTCTCATATTCAT-3' Rev), PDGFR β (5'-CCGGAACAAACACACCTTCT-3' FW; 5'-AACATGGGCACGTAATC TATA-3' Rev), Sca1 (5'-TTACCCATCTGCCCTCTAA-3' FW; 5'-GGTCTGCAG GAGGATGAGC-3' Rev), α SMA (5'-CTGACAGAGGCACCAGTAA-3' FW; 5'-C ATCTCCAGATCCAGCACA-3' Rev), Pax7 (5'-GACTCGGCTTCTCCATCTC-3' FW; 5'-AGTAGGCTTGCCCGTTCC-3' Rev), VE cadherin (5'-GTACAGCATCATG CAGGGCG-3' FW; 5'-ATTCGTATCGGATAGTGGGG-3' Rev), Smoothelin (5'-A TCTGATTCTCCCGTGGTTG-3' FW; 5'-CTGCTTCTGTGGGAGGAAG-3' Rev), smMHC (5'-GCAGAAGGCTCAGACCAAAG-3' FW; 5'-TATCCAGAATGCCAGGAA G-3' Rev), msx2 (5'-CCATATACGGCGCATCTACC-3' FW; 5'-CAACCGGCTGGC ATAGAG-3' Rev), aP2 (5'-TCACCTGGAAGACAGCTCT-3' FW; 5'-AATCCCATTT ACCTGTATG-3' Rev), PPAR γ (5'-AGACAACGGACAATACCA-3' FW; 5'-TGGAC ACCATCTTGCAGCA-3' Rev), MyoD (5'-ACGGCTCTCTCTGCTCCTT-3' FW; 5'-GTAGGGAAGTGTGCGTGT-3' Rev), Myogenin (5'-GATCCCCCTATTTT TACCA-3' FW; 5'-GTCCCAAGTCCCTTTTCTTCC-3' Rev), MHC (5'-GGCCAAATC AAAGAGGTGA-3' FW; 5'-CGTGCTTCTCTCTCAACC-3' Rev), GFP (5'-ACAAG CAGAAGAACGGCATC-3' FW; 5'-CGGTACGAACTCCAGCA-3' Rev), α -SG (5'-C TTGTGGTCTGTGTTGT-3' FW; 5'-GGTGAGCGTGGTAGGTGAGT-3' Rev).

Quantification has been performed using the Δ Ct method using as reference gene cyclophilin A or GAPDH, or the Livak method for relative gene expression analysis, using as reference value the value of wt MABs or GFPMABs.

Chromatin immunoprecipitation. ChIP assay was performed as previously described¹⁰ on 6×10^6 of overexpressing Necdin MABs grown in differentiating medium for 3 days.

The input DNA was an aliquot of the supernatant from the centrifuged sonicate (DNA size range: 200–1000 bp). The chromatin was immunoprecipitated with normal rabbit IgG (Santa Cruz Biotechnology, Santa Cruz, CA, USA), rabbit anti-HA (Santa Cruz Biotechnology) and rabbit anti-necdin (Upstate Biotechnology, Waltham, MA, USA). PCRs were performed on the purified immunoprecipitated DNA with GoTaq (Promega) and the primers used were myogenin (5'-GAATCACATGTAATCCACTGGA-3' FW, 5'-ACGCCAACTGCTGGGTGCCA-3' REV) and β -actin (5'-GCTCTTTGCAGCTC TTCTGTTG-3' FW, 5'-TTTGACATGCCGGAGCCGTTGT-3' REV).

Cell resistance to cell death. MABs from the different genotypes were incubated with or without 2 μ M staurosporine for 3 h or with or without 20 μ M As₂O₃ overnight. Cells were detached and stained with PI according to the kit's manufacturer's instructions and analyzed by flow cytometry as described.²⁴

Protein extracts and immunoblot analysis. Muscles tissue were homogenized or cells were scraped in 20 mM Tris-HCl pH 8.8, 5 mM EDTA, 10% glycerol, 50 mM NaF, 1% Triton X-100 and protease inhibitor cocktail (Sigma) and centrifuged for 10 min at 13 000 r.p.m. at 4°C to discard cellular debris. After electrophoresis, proteins (30–40 μ g) were electrophoretically transferred onto nitrocellulose filters and antigens revealed by the respective primary Abs and the appropriate secondary Abs, as already described.¹⁰ The antibodies used were anti-Necdin (Upstate Biotechnology), anti-MyoD (Dako, Carpinteria, CA, USA), anti-sarcomeric myosin MF20 and anti-myogenin (from Developmental Studies Hybridoma Bank), anti- α -SG (Novocastra) and, to normalize protein levels, anti- β -tubulin (Covance, Emeryville, CA, USA) and anti-glyceraldehyde 3-phosphate dehydrogenase (GAPDH) mAb (Biogenesis, Poole, UK).

In-vivo transplantation. Four-month-old α -SG^{-/-} mice were injected by intramuscular delivery with 5×10^5 (for TA) or with 7×10^5 mouse MABs (for quadriceps and gastrocnemius) and animals were killed 14 days after transplantation. Different muscles were collected for real-time PCR or frozen in isopentane cooled by liquid nitrogen for histological analysis.

In-vivo cell survival assay. To identify MABs undergoing apoptosis *in vivo*, we performed, together with GFP immunofluorescence, TUNEL test using the ApopTag Red *In Situ* Apoptosis Detection Kit (Chemicon International) according to the manufacturer's instructions, on cryostat sections of OCT-embedded muscles of α -SG^{-/-} mice recovered 24 h after MABs intramuscular injection.

Tissue digestion and flow cytometric analysis of cell death. Muscles of α -SG^{-/-} mice were recovered 24 h after MABs intramuscular injection and finely minced. Each sample underwent four cycles of enzymatic digestion at 37°C for 10 min in the presence of 3.5 mg/ml dispase (Invitrogen) and 0.5 mg/ml collagenase type V (Sigma). The single cell suspension was filtered to remove tissue debris. The isolated cells were harvested and resuspended in PBS 10% FBS. Cells were stained with 10 μ g/ml of 7AAD (Sigma-Aldrich). Cell analysis was performed on at least 10 000 events for each sample and determined using the Accuri C6 Flow Cytometer System. The analysis was performed using the Accuri CFlow software. A primary gate based on the physical parameters (forward and side light scatter, FSC and SSC, respectively) was set to exclude dead cells or small debris.

Image acquisition and manipulation. Images in fluorescence and phase contrast have been taken on the Nikon microscope Eclipse E600 (Nikon Instruments S.p.a., Firenze, Italy) (lenses Plan Fluor: $\times 4/013$, $\times 10/0.33$, $\times 20/0.50$, $\times 40/0.75$), or on the Leica AF6000 (Leica Microsystems GmbH, Wetzlar, Germany). Images have been acquired using the Nikon digital camera DXM1200 (Nikon Instruments S.p.a.), and the acquisition software NIKON ACT-1, or using the DFC350 FX digital camera (Nikon Instruments S.p.a.) and the Leica AF600 acquisition software (Leica Microsystems GmbH), imaging medium, PBS buffer, room temperature. Images were assembled in panels using Adobe Photoshop 7.0 (Adobe Systems Inc., San Jose, CA, USA). Images showing double fluorescence were first separately acquired using the different appropriate filters, the two layers then merged with Adobe Photoshop 7.0.

Acknowledgements. This work has benefited from research funding from Telethon (GGP07013), the Italian Ministry of University and Research (PRIN 2009), the European Community's Seventh Framework Programme in the project ENDOSTEM (Grant agreement number 241440) to SB, and OPTISTEM (Grant agreement number 223098) to GC. We are also grateful to Jordi Diaz-Manera for technical help.

- Zammit PS, Partridge TA, Yablonka-Reuveni Z. The skeletal muscle satellite cell: the stem cell that came in from the cold. *J Histochem Cytochem* 2006; **54**: 1177–1191.
- Conboy IM, Rando TA. Aging, stem cells and tissue regeneration: lessons from muscle. *Cell Cycle* 2005; **4**: 407–410.
- Minasi MG, Riminucci M, De Angelis L, Borello U, Berarducci B, Innocenzi A *et al*. The meso-angioblast: a multipotent, self-renewing cell that originates from the dorsal aorta and differentiates into most mesodermal tissues. *Development* 2002; **129**: 2773–2783.
- Sampaolesi M, Blot S, D'Antona G, Granger N, Tonlorenzi R, Innocenzi A *et al*. Mesoangioblast stem cells ameliorate muscle function in dystrophic dogs. *Nature* 2006; **444**: 574–579.
- Sampaolesi M, Torrente Y, Innocenzi A, Tonlorenzi R, D'Antona G, Pellegrino MA *et al*. Cell therapy of alpha-sarcoglycan null dystrophic mice through intra-arterial delivery of mesoangioblasts. *Science* 2003; **301**: 487–492.
- Barker PA, Salehi A. The MAGE proteins: emerging roles in cell cycle progression, apoptosis, and neurogenetic disease. *J Neurosci Res* 2002; **67**: 705–712.
- Cassidy SB. Prader-Willi syndrome. *J Med Genet* 1997; **34**: 917–923.
- Gerard M, Hernandez L, Wevrick R, Stewart CL. Disruption of the mouse necdin gene results in early post-natal lethality. *Nat Genet* 1999; **23**: 199–202.

- Muscattelli F, Abrus DN, Massacrier A, Boccaccio I, Le Moal M, Cau P *et al*. Disruption of the mouse Necdin gene results in hypothalamic and behavioral alterations reminiscent of the human Prader-Willi syndrome. *Hum Mol Genet* 2000; **9**: 3101–3110.
- Deponti D, Francois S, Baesso S, Sciorati C, Innocenzi A, Broccoli V *et al*. Necdin mediates skeletal muscle regeneration by promoting myoblast survival and differentiation. *J Cell Biol* 2007; **179**: 305–319.
- Kuwajima T, Taniura H, Nishimura I, Yoshikawa K. Necdin interacts with the Msx2 homeodomain protein via MAGE-D1 to promote myogenic differentiation of C2C12 cells. *J Biol Chem* 2004; **279**: 40484–40493.
- Sciorati C, Touvier T, Buono R, Pessina P, Francois S, Perrotta C *et al*. Necdin is expressed in cachectic skeletal muscle to protect fibers from tumor-induced wasting. *J Cell Sci* 2009; **122** (Part 8): 1119–1125.
- Pessina P, Conti V, Pacelli F, Rosa F, Doglietto GB, Brunelli S *et al*. Skeletal muscle of gastric cancer patients expresses genes involved in muscle regeneration. *Oncol Rep* 2010; **24**: 741–745.
- Tonlorenzi R, Dellavalle A, Schnapp E, Cossu G, Sampaolesi M. Isolation and characterization of mesoangioblasts from mouse, dog, and human tissues. *Curr Protoc Stem Cell Biol* 2007; Chapter 2: Unit 2B.1.
- Brunelli S, Tagliafico E, De Angelis FG, Tonlorenzi R, Baesso S, Ferrari S *et al*. Msx2 and necdin combined activities are required for smooth muscle differentiation in mesoangioblast stem cells. *Circ Res* 2004; **94**: 1571–1578.
- Dellavalle A, Sampaolesi M, Tonlorenzi R, Tagliafico E, Sacchetti B, Perani L *et al*. Pericytes of human skeletal muscle are myogenic precursors distinct from satellite cells. *Nat Cell Biol* 2007; **9**: 255–267.
- Brunelli S, Rovere-Querini P. The immune system and the repair of skeletal muscle. *Pharmacol Res* 2008; **58**: 117–121.
- Peault B, Rudnicki M, Torrente Y, Cossu G, Tremblay JP, Partridge T *et al*. Stem and progenitor cells in skeletal muscle development, maintenance, and therapy. *Mol Ther* 2007; **15**: 867–877.
- Cossu G, Biressi S. Satellite cells, myoblasts and other occasional myogenic progenitors: possible origin, phenotypic features and role in muscle regeneration. *Semin Cell Dev Biol* 2005; **16**: 623–631.
- Gargioli C, Coletta M, De Grandis F, Cannata SM, Cossu G. PIGF-MMP-9-expressing cells restore microcirculation and efficacy of cell therapy in aged dystrophic muscle. *Nat Med* 2008; **14**: 973–978.
- Brunelli S, Sciorati C, D'Antona G, Innocenzi A, Covarello D, Galvez BG *et al*. Nitric oxide release combined with nonsteroidal antiinflammatory activity prevents muscular dystrophy pathology and enhances stem cell therapy. *Proc Natl Acad Sci USA* 2007; **104**: 264–269.
- Donati C, Cencetti F, De Palma C, Rapisardi E, Brunelli S, Cossu G *et al*. TGFbeta protects mesoangioblasts from apoptosis via sphingosine kinase-1 regulation. *Cell Signal* 2009; **21**: 228–236.
- Palumbo R, Galvez BG, Pusterla T, De Marchis F, Cossu G, Marcu KB *et al*. Cells migrating to sites of tissue damage in response to the danger signal HMGB1 require NF-kappaB activation. *J Cell Biol* 2007; **179**: 33–40.
- Sciorati C, Galvez BG, Brunelli S, Tagliafico E, Ferrari S, Cossu G *et al*. *Ex vivo* treatment with nitric oxide increases mesoangioblast therapeutic efficacy in muscular dystrophy. *J Cell Sci* 2006; **119** (Part 24): 5114–5123.
- Galvez BG, Sampaolesi M, Brunelli S, Covarello D, Gavina M, Rossi B *et al*. Complete repair of dystrophic skeletal muscle by mesoangioblasts with enhanced migration ability. *J Cell Biol* 2006; **174**: 231–243.
- Zhu N-L, Wang J, Tsukamoto H. The Necdin-Wnt pathway causes epigenetic peroxisome proliferator-activated receptor gamma repression in hepatic stellate cells. *J Biol Chem* 2010; **285**: 30463–30471.
- Tseng Y-H, Butte AJ, Kokkotou E, Yechoor VK, Taniguchi CM, Kriauciunas KM *et al*. Prediction of preadipocyte differentiation by gene expression reveals role of insulin receptor substrates and necdin. *Nat Cell Biol* 2005; **7**: 601–611.
- Uezumi A, Fukada S-i, Yamamoto N, Takeda Sai, Tsuchida K. Mesenchymal progenitors distinct from satellite cells contribute to ectopic fat cell formation in skeletal muscle. *Nat Cell Biol* 2010; **12**: 143–152.
- Biressi S, Rando TA. Heterogeneity in the muscle satellite cell population. *Semin Cell Dev Biol* 2010; **21**: 845–854.
- Hoshiya H, Kazuki Y, Abe S, Takiguchi M, Kajitani N, Watanabe Y *et al*. A highly stable and nonintegrated human artificial chromosome (HAC) containing the 2.4 Mb entire human dystrophin gene. *Mol Ther* 2009; **17**: 309–317.
- Weber J. Immunotherapy for melanoma. *Curr Opin Oncol* 2011; **23**: 163–169.
- Chapman EJ, Knowles MA. Necdin: a multi functional protein with potential tumor suppressor role? *Mol Carcinog* 2009; **48**: 975–981.
- Tagliafico E, Brunelli S, Bergamaschi A, De Angelis L, Scardigli R, Galli D *et al*. TGF[beta]/BMP activate the smooth muscle/bone differentiation programs in mesoangioblasts. *J Cell Sci* 2004; **117** (Part 19): 4377–4388.

Supplementary Information accompanies the paper on Cell Death and Differentiation website (<http://www.nature.com/cdd>)